Optics Communications 285 (2012) 3820–3826

Contents lists available at SciVerse ScienceDirect

Optics Communications

journal homepage: www.elsevier.com/locate/optcom

Photon time-interval statistics applied to the analysis of laser heterodyne signal with photon counter

Lisheng Liu [a,b,*], Heyong Zhang [a,b], Jin Guo [a], Shuai Zhao [a], Tingfeng Wang [a]

[a] State Key Laboratory of Laser Interaction with Matter, Changchun Institute of Optics, Fine Mechanics and Physics, Chinese Academy of Science, Changchun 130033, China
[b] Graduate University of Chinese Academy of Sciences, Beijing 100039, China

ARTICLE INFO

Article history:
Received 18 October 2011
Received in revised form
8 February 2012
Accepted 11 May 2012
Available online 2 June 2012

Keywords:
Laser heterodyne signal
Photon counter
Photon time-interval
Probability density function
Mixing efficiency

ABSTRACT

In this paper, we report a mathematical derivation of probability density function (PDF) of time-interval between two successive photoelectrons of the laser heterodyne signal, and give a confirmation of the theoretical result by both numerical simulation and an experiment. The PDF curve of the beat signal displays a series of fluctuations, the period and amplitude of which are respectively determined by the beat frequency and the mixing efficiency. The beat frequency is derived from the frequency of fluctuations accordingly when the PDF curve is measured. This frequency measurement method still works while the traditional Fast Fourier Transform (FFT) algorithm hardly derives the correct peak value of the beat frequency in the condition that we detect 80 MHz beat signal with 8 Mcps (counts per-second) photons count rate, and this indicates an advantage of the PDF method.

1. Introduction

As a new technique for laser coherent detection, the application of singe-photon counter for coherent laser radar is proposed by Lincoln Laboratory in recent years [1]. The detector they used is avalanche photodiode (APD) operating in Geiger-mode, which is a method for operating an APD at a reverse bias higher than the breakdown voltage [2]. The main benefit of the Geiger-mode APD is the ability to be used in large-format arrays, which yields excellent photon counting characteristic and also can be used for imaging [3,4]. And the compactness, robustness, low cost, low operating voltage and power consumption are also added values against traditional photodetectors [5–7]. In Lincoln Laboratory, they have put forward a simple technique to mitigate impact of turbulence on heterodyne laser radar based on photon-counting detector arrays and analyze saturation effects in heterodyne detection with Geiger-mode InGaAs APD arrays [8]. For laser heterodyne using, the Geiger-mode APD arrays registers photons arrival times [9], and a FFT of the times can map out beat frequency of laser heterodyne signal.

In this paper, we focus on the PDF of photons time-interval of arrival to analyze laser heterodyne signal. The time-interval of photons is often used in low light intensity levels [10,11] and has a wide application in physics, astronomy and chemistry, for example, to analyze squeezed light [12], degenerate optical parametric oscillator [13], atomic state reduction in resonance fluorescence [14], laser-pulse-timing fluctuations [15], solar flare hard X-ray bursts [16] and molecular interactions [17] etc.

It is well known that the photon detection is a Binomial process, and when the expected number of detection occurring within the finite time-interval Δt is given, the probability of the photons number lying in the same time-interval Δt obeys Poisson distribution [18]. In this paper, based on the Poisson distribution, we derived the PDF of time-interval between two successive photoelectrons of stationary light signal and laser heterodyne signal [19], and it has found some special characteristics in the PDF curve of the beat signal, which can be used to obtain the beat frequency and estimate the mixing efficiency.

2. The PDF of time-interval

The photon counting detector that collects the incident photons is a square-law detector and the resulting current is a sum of delta functions, where each delta function corresponds to a photoelectron event. In order to discuss the time-interval distribution for a light beam we need the probability of the photoelectron events number in a certain time period. For simplification and to get an ideal model, we shall not take the impact of afterpulsing into account, which occurs when the generated carriers are trapped by crystal defects [20]. In the ideal model, the probability of detecting k photoelectric events in

* Corresponding author at: State Key Laboratory of Laser Interaction with Matter, Changchun 130033, China. Tel.: +86 15164311891.
E-mail address: liulishengz@yahoo.com.cn (L. Liu).

0030-4018/$ - see front matter © 2012 Elsevier B.V. All rights reserved.
http://dx.doi.org/10.1016/j.optcom.2012.05.019

$[t, t+\tau]$ is [21]

$$P(k,t,\tau)=\frac{1}{k!}[\eta\int_t^{t+\tau}I(t')dt']^k\exp\left[-\eta\int_t^{t+\tau}I(t')dt'\right] \quad (1)$$

where $I(t)$ is the instantaneous intensity of the signal light and η is the detection efficiency depending on the characteristics of the detector. We find from Eq. (1) that the probability that no photoelectron occurs in the interval $[t, t+\tau]$ is

$$P(0,t,\tau)=\exp[-\eta\int_t^{t+\tau}I(t')dt'] \quad (2)$$

and the probability of detecting one photon in a short interval $[t-\Delta t, t]$ is found to be

$$P(1,t-\Delta t,t)=\eta\int_{t-\Delta t}^{t}I(t')dt'\exp[-\eta\int_{t-\Delta t}^{t}I(t')dt'] \approx\eta I(t)\Delta t \quad (3)$$

in which $\eta I(t)=N(t)$ is the photons count rate. From Eqs. (2) and (3) we obtain the joint probability of detection one photon in $[t-\Delta t, t]$, no photon in $[t, t+\tau]$, and one photon in the interval $[t+\tau, t+\tau+\Delta\tau]$ to be [12]

$$P^{(3)}(1,t-\Delta t,t;0,t,t+\tau;1,t+\tau,t+\tau+\Delta\tau) =\eta^2 I(t)\exp[-\eta\int_t^{t+\tau}I(t')dt']I(t+\tau)\Delta t\Delta\tau \quad (4)$$

We may look on the conditional probability

$$P_C(\tau)=\frac{P^{(3)}(1,t-\Delta t,t;0,t,t+\tau;1,t+\tau,t+\tau+\Delta\tau)}{P(1,t-\Delta t,t)} \quad (5)$$

of registering a detection at time $t+\tau$ within $\Delta\tau$, given a detection at time t, as an expression for the distribution of the time-interval τ between successive photons. The time-interval PDF $p(\tau)$ for two successive photoelectrons to be separated by the time-interval τ is then

$$p(\tau)=\lim_{\Delta\tau\to 0}\frac{P_C(\tau)}{\Delta\tau}=\eta\exp(-\eta\int_t^{t+\tau}I(t')dt')I(t+\tau) \quad (6)$$

which is the basic formula used later to derive the time-interval PDF for laser heterodyne signal.

In the particularly simple case in which the field is in a coherent state, with the light intensity $I(t)$ constant at all time, and $\eta I(t)=N$ is the average count rate, it follows from Eq. (6) that

$$p_{Stationary}(\tau)=Ne^{-N\tau} \quad (7)$$

which is called negative exponential distribution, and represent the time-interval PDF of stationary light signal.

2.1. Time-interval PDF for laser heterodyne signal

The beam intensity containing beat signal can be written directly as

$$I_{Beat}(t)=I_{LO}+I_S+2m\sqrt{I_{LO}I_S}\cos(2\pi f_{IF}t+\theta) \quad (8)$$

where I_{LO} and I_S are the DC contribution from the local oscillator and signal beams, third term is contribution of beat signal, where m is the mixing efficiency, f_{IF} is the intermediate frequency given by $|f_{LO}-f_S|$, and θ is the initial phase given by $\theta_{LO}-\theta_S$.

Since the photoelectron is directly proportional to the signal intensity, the detected photons arrival times must contain periodic component because of the periodicity of the signal intensity as shown in the last term of Eq. (8). The relationship of beat signal and photons arrival times is shown in Fig. 1. in which, every upright line represents a photoelectron event, the interspaces of two successive lines represent time-interval. And we can see from Fig. 1 that more photons are detected when the beat signal wave crest arrives, and the time-interval is small; when the wave trough arrives, there are less photons and large time-interval.

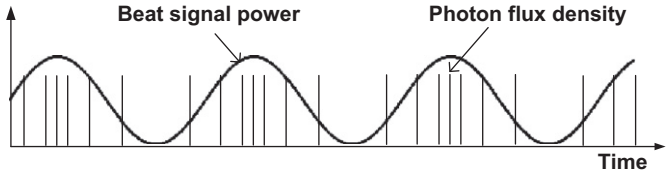

Fig. 1. Histogram of arrival times of detected photons traces out beat frequency signal.

Making use of Eqs. (6) and (8), we product the conditional time-interval PDF of the beat signal as

$$p_{Beat}(\tau|t)=\eta\exp(-\eta\int_t^{t+\tau}I_{Beat}(t')dt')\times I_{Beat}(t+\tau) \quad (9)$$

in the condition that photoelectron events occur at a given time t. However, when an experiment is carried on, our recording data lays in a period of time as $[0, T]$, and the time-interval PDF independent of t can be derived by

$$p_{Beat}(\tau)=\int_0^T p_{Beat}(\tau|t)p_{time}(t)dt \quad (10)$$

where $p_{time}(t)$ is the PDF of the photons arrival times, which is directly proportion to the beat signal intensity (see Fig. 1) and written as

$$p_{time}(t)\propto I_{LO}+I_S+2m\sqrt{I_{LO}I_S}\cos(2\pi f_{IF}t+\theta) \quad (11)$$

The PDF for photons arrive times can be found by normalizing Eq. (11) so that it integrates to 1 over the detection time T [1,18], yielding

$$p_{time}(t)=\frac{I_{LO}+I_S+2m\sqrt{I_{LO}I_S}\cos(2\pi f_{IF}t+\theta)}{(I_{LO}+I_S)T+(m\sqrt{I_{LO}I_S}/\pi f_{IF})[\sin(2\pi f_{IF}T+\theta)-\sin\theta]} \quad (12)$$

we substitute Eqs. (8), (9) and (12) into Eq. (10), and get an equation

$$\begin{aligned}p_{Beat}(\tau)=\exp[-(N_S+N_{LO})\tau]/\Bigg\{&(N_S+N_{LO})T\\&+\frac{m\sqrt{N_SN_{LO}}}{\pi f_{IF}}\left[\sin(2\pi f_{IF}T+\theta)-\sin\theta\right]\Bigg\}\\&\times\int_0^T\left\{\left\{N_S+N_{LO}+2m\sqrt{N_SN_{LO}}\cos\left[2\pi f_{IF}(t+\tau)+\theta\right]\right\}\right.\\&\times\exp\left\{-\frac{m\sqrt{N_SN_{LO}}}{\pi f_{IF}}\sin\left[2\pi f_{IF}(t+\tau)+\theta\right]\right\}\\&\times\left[N_S+N_{LO}+2m\sqrt{N_SN_{LO}}\cos(2\pi f_{IF}t+\theta)\right]\\&\left.\times\exp\left[\frac{m\sqrt{N_SN_{LO}}}{\pi f_{IF}}\sin(2\pi f_{IF}t+\theta)\right]\right\}dt\end{aligned} \quad (13)$$

which is the ultimate conclusion in this paper, unfortunately has no simple analytical expression and can be plotted with numerical method.

The intensity of laser heterodyne signal can be transformed into photons count rate using

$$N_{Beat}(t)=\eta I_{Beat}(t)$$

which will be used in the next numerical calculation.

3. Numerical calculation

Before proceeding, it is important to make discussion of the length of detection time period $[0, T]$. If T is smaller than one period of the beat signal, the initial phase θ will have a significant

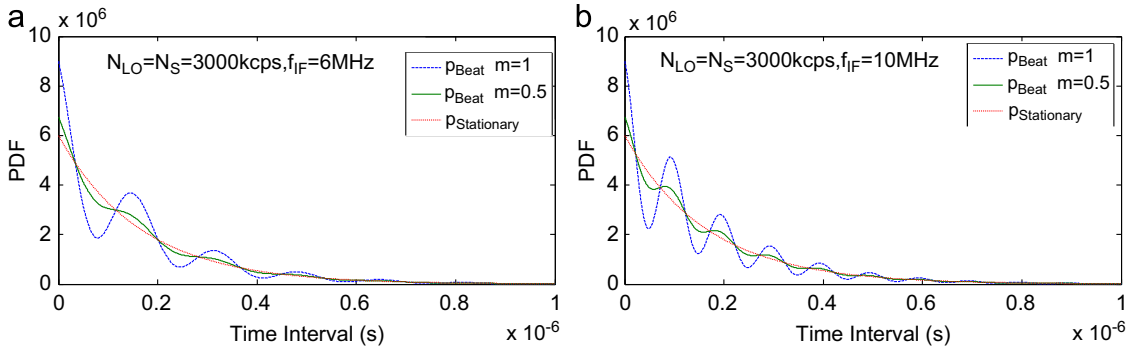

Fig. 2. PDF of time-interval at f_{IF}=6 MHz (a) and f_{IF}=10 MHz (b). For p_{Beat}, $N_{LO}=N_S$=3000 kpcs, and for $p_{Stationary}$, $N=N_{LO}+N_S$=6000 kcps.

impact on the shape of the PDF graph because we only detect a portion of one beat period. If T is far larger than one beat period, in which case, we detect abundant complete beat periods, and the influence of the first partial period is drowned out. And this is the case in our experiment, so the initial phase θ is neglected in the numerical calculation.

Eq. (13) is plotted in Fig. 2 for two intermediate frequencies of f_{IF}=6 MHz and 10 MHz and two mixing efficiencies of m=0.5 and 1. In order to distinguish the difference between stationary light beam and beat signal beam, the negative exponential distribution Eq. (7) is also plotted in the same figure in condition that photons count rate is the sum of local oscillator and signal as $N=N_{LO}+N_S$.

In Fig. 2, the time-interval PDF curves of the beat signal exhibit significant difference from that of stationary signal, the later attenuates smoothly as the increment of time-interval obeying negative exponential distribution, while the former attenuates with fluctuations on the PDF curves. From the comparison of m=0.5 and 1, we find a bigger mixing efficiency produces a larger fluctuation amplitude. Compared the two PDF curves of different intermediate frequencies of f_{IF}=6 MHz and 10 MHz, we find that there are more fluctuations for larger f_{IF}. As Fig. 2 shown, there are 6 fluctuation periods for 6 MHz within 1 μs time-interval, and 10 periods for 10 MHz. The frequency of these fluctuations corresponding to the time-interval in the abscissa axis is the beat frequency. The fluctuations in the curves can be understood as: in Fig. 1, the periodic change of the beat signal intensity drives photons arrival times changing periodically, as a result, the time-interval between two successive photons exists periodic characteristic which is denoted in its PDF graph.

These characteristics of the PDF curve reflect two information of the beat signal: the mixing efficiency and the beat frequency. And both can be obtained simultaneously if we measured the PDF of laser heterodyne signal.

To derive the beat frequency more conveniently, we define the parameter $\rho(\tau)$ given by

$$\rho(\tau)=\frac{p_{Beat}(\tau)}{p_{Stationary}(\tau)} \tag{14}$$

and plotted in Fig. 3.

The parameter $\rho(\tau)$ changes cosinoidal with time-interval, and the cosine wave frequency is the beat frequency. It is important to make clear again that the abscissa axis in Fig. 3 is time-interval between two successive photons, but not time. In the beat frequency measurement experiment using this method, our procedures are as follows: 1. Register beat signal photons arrival times. 2. Deal with the time-interval to derive its PDF. 3. Get the ratio of beat signal PDF to negative exponential distribution calculated using $N=N_{LO}+N_S$. The ratio parameter $\rho(\tau)$ frequency is the beat frequency.

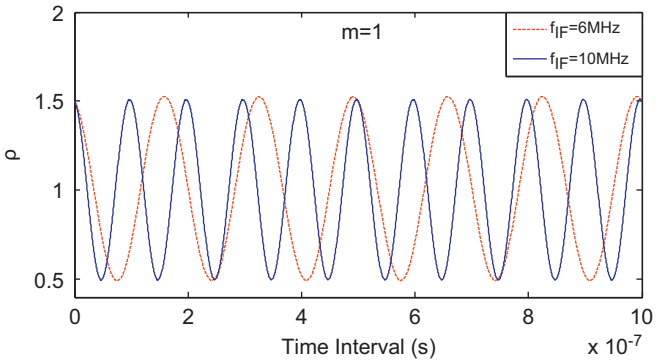

Fig. 3. The ratio of p_{Beat} to $p_{Stationary}$ at f_{IF}=6 MHz and f_{IF}=10 MHz when m=1.

3.1. Influence of photons count rate

The expectation of stationary signal time-interval can be calculated by

$$E_{Stationary}(\tau)=\int_0^\infty \tau p_{Stationary}(\tau)d\tau=\frac{1}{N} \tag{15}$$

Because there is no analytical expression for Eq. (13), the expectation of beat signal time-interval must be calculated numerically, and fortunately we find it has the same formula as stationary signal,

$$E_{Beat}(\tau)=\frac{1}{N_{LO}+N_S} \tag{16}$$

which indicates stationary and beat signal have the same expectation when photons count rate is equal. Eqs. (15) and (16) also indicate that the time-interval is inversely proportion to photons count rate.

As the graph shown in Fig. 2, when the value of time-interval is large, the PDF value is small and the fluctuations are not as evident as little value, and it will produce a bigger measurement error. Therefore, we need to define a time-interval upper limit τ_{max} and the data exceeding τ_{max} could be ignored. Based on substantive numerical calculation, an empirical τ_{max} is give by

$$\tau_{\max}=3E(\tau) \tag{17}$$

The probability for time-interval below τ_{max} is

$$P_{Stationary}(\tau<3E(\tau))=P_{Beat}(\tau<3E(\tau))=95.02\% \tag{18}$$

And it shows the time-interval locates in [0, $3E(\tau)$] with the probability of 95%.

In order to derive the beat frequency, there is at least one fluctuation period existing in the PDF curve. Figs. 2 and 3 have

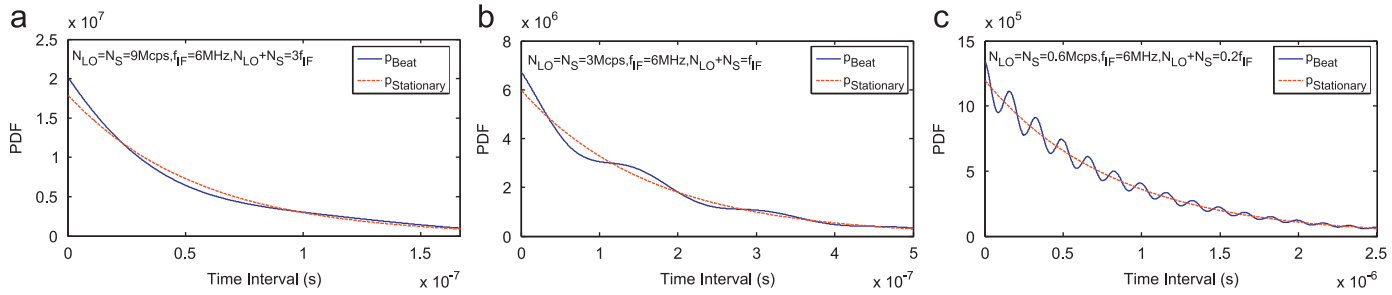

Fig. 4. The PDF of beat frequency of 6 MHz of various photons count rates. And the respective count rate is $N_{LO}+N_S=18$, 6 and 1.2 Mcps, corresponding to 3, 1, and 0.2 times the values of beat frequency.

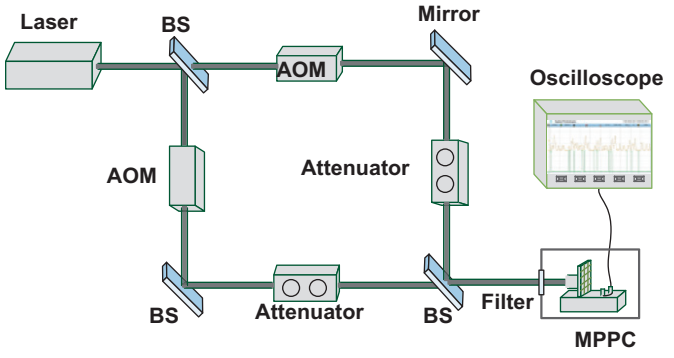

Fig. 5. Experiment setup for validating of the presented theory.

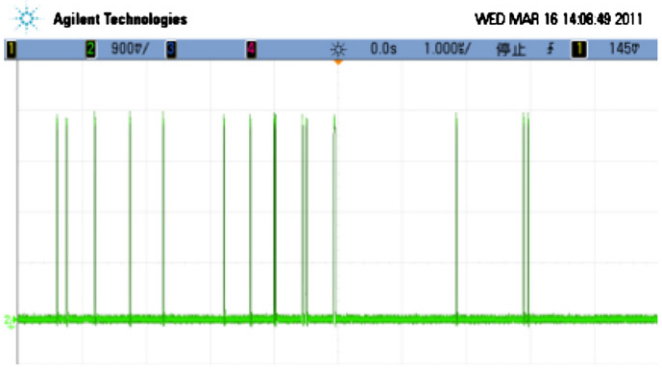

Fig. 6. Output of the MPPC module.

exhibited the fluctuation frequency which is directly proportion to the beat frequency, so there is equation

$$3E(\tau)=\frac{3}{N_S+N_{LO}}\geq\frac{1}{f_{IF}} \tag{19}$$

which satisfies that at least one fluctuation is observed. Then

$$N_S+N_{LO}\leq 3f_{IF} \tag{20}$$

indicating that the upper limit photons count rate is treble numerical value of the frequency, and when the experiment is carried on, the photons count rate cannot exceed $3f_{IF}$. The PDF curves within τ_{max} are plotted for various photons count rates in Fig. 4.

Fig. 14 shows that more fluctuations exist in the PDF curves because of large time-interval shown in the abscissa axis produced by little count rate. We hope to observe more fluctuations in the PDF curves to achieve good measurement accuracy, so little photons count rate will be adopted in experiment. Note that, the maximum value in the abscissa axis in Fig. 4 is $3E(\tau)$, which is the τ_{max} we have defined. Since the probability of time-interval lying in $[0, 3E(\tau)]$ is 95%, we think it is a reasonable limit.

4. Experimental verification

To verify the theory present in the former section, we perform an experiment with system setup shown in Fig. 5.

We use the Nd:YAG laser source with 532 nm wavelength and 1 MHz bandwidth, the beam is split into two by the beam splitter. One of the beams is modulated by an AOM with 80 MHz frequency shift and is regarded as local oscillator, the other is regarded as signal beam modulated by another AOM whose center frequency shift is 80 MHz and has an accommodate range of $\pm$20 MHz. Two tunable attenuators are used before mixing of two beams to limit the beam intensity to safe value of the detector and make the two beams match each other ($N_{LO}=N_S$).

The detector we used is multi-pixel photon counter (MPPC) module made by Hamamatsu in Japan whose product has been used in [22,23]. The MPPC module has 1600 pixels and 20 ns dead time. It offers various thresholds to reduce dark count noise and the dark count rate is typical 500 kcps at a threshold of 0.5 p.e. at the room temperature. In our system setup, we insert a 532 nm wavelength filter of 1 nm bandwidth to reduce surrounding noise. A radiator is put into the encapsulation of MPPC module to make it work at a surrounding temperature of about 10 °C. The MPPC output is shown in Fig. 6, every δ pulse corresponds to a photoelectron event, and the photons arrival times are recorded.

4.1. Stationary light

First, we only register photons arrival times of local oscillator beam to verify Eq. (7) which is the time-interval PDF of stationary signal. 74,760 photoelectron events are recorded in the detection time of 40 ms, and the photons count rate can be calculated to 1.869 Mcps and the mean value of time-interval is 0.535 μs. We process the time-interval and derive its PDF shown in Fig. 7. It can be found that the measured data is in good agreement with theoretical curve.

4.2. Beat signal

The frequency shift of the signal beam is tuned to be 72 MHz by the AOM resulting in an 8 MHz beat frequency. The respective photons count rates of local and signal beams are set equal. We select various MPPC thresholds to make photons count rates to be about 1, 0.5 and 0.2 times numerical values of the beat frequency, and the mean value of time-interval is calculated using Eq. (16), and we only deal with the data under $3E(\tau)$. The results are shown in Figs. 8 and 9.

First of all, we make a point clear that our experiment does not contain the data lying in [0 ns, 20 ns] because of the 20 ns dead

time leads that MPPC records a minimum time-interval of 20 ns. We find that the measured data follows the theoretical calculation quite well at little count rate, but deviates from theory at large count rate. This could be due to dark count noise when a small MPPC threshold is selected. Using this measurement results, we can not only derive the beat frequency from the fluctuation frequency, but also obtain an estimation of the mixing efficiency, which is about 0.65 over here.

4.3. Dark noise

One drawback of MPPC is high dark count rate [24]. One noise photon exists, it will cause two noise time-interval arise and one signal time-interval dropout (see Fig. 10). We will discuss the influence of the dark noise from the aspect of false alarm.

According to the decision rule in [25]

$$l(\tau)=\frac{p_{Signal}(\tau)}{p_{Noise}(\tau)}\geq\frac{P(\text{Noise})}{P(\text{Signal})} \tag{21}$$

where $l(\tau)$ is called likelihood ratio, when it satisfies Eq. (21), we think a signal is present. In Eq. (21) there is the relationship

$$\frac{P(\text{Noise})}{P(\text{Signal})}=\frac{N_{Noise}}{N_{Signal}} \tag{22}$$

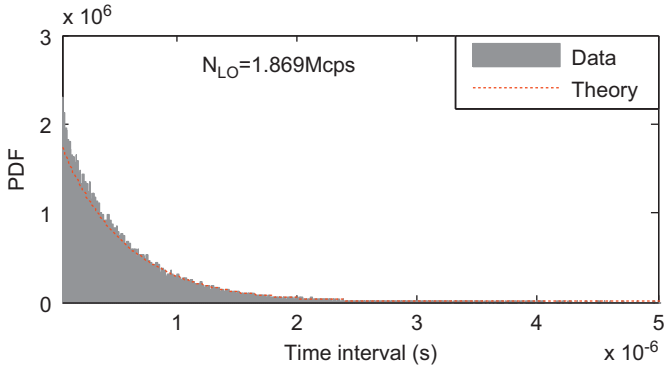

Fig. 7. Measured PDF of stationary signal at photons count rate of 1.869 Mcps.

Because dark count of the MPPC obeys Poisson distribution (see Fig. 11), its time-interval PDF is the same as Eq. (7). That is

$$p_{Noise}(\tau)=N_{Noise}e^{-N_{Noise}\tau} \tag{23}$$

For stationary signal, this likelihood ratio $l(\tau)$ is a monotonic function of τ, and there is only one feasible region for the in Eq. (21). We can easily obtain the solution

$$\tau\leq\tau_s=2\ln\left(\frac{N_{Noise}}{N_{Signal}}\right)(N_{Noise}-N_{Signal}) \tag{24}$$

Then the false alarm is given by

$$P_{\text{FA}}=\int_0^{\tau_s}p_{Noise}(\tau)d\tau \tag{25}$$

But for beat signal, $l(\tau)$ is not a monotonic function, and there are more than one feasible regions (see Fig. 12), written as

$$0\leq\tau\leq\tau_s^{(1)},\tau_s^{(2)}\leq\tau\leq\tau_s^{(3)},\cdots \tag{26}$$

The false alarm is derived by integration of all the regions, given by

$$P_{FA}=\int_0^{\tau_s^{(1)}}p_{\text{Noise}}(\tau)d\tau+\int_{\tau_s^{(2)}}^{\tau_s^{(3)}}p_{\text{Noise}}(\tau)d\tau+\cdots \tag{27}$$

Given the measurement data used in Figs. 8 and 9, where the beat frequency is 8 MHz, we calculated the ratio of N_{Signal} to N_{Noise} and the false alarm under the condition of various MPPC thresholds. List in Table 1.

The ratio and the false alarm are plotted in Fig. 13.

It shows that large MPPC threshold results in large ratio of N_{Signal} to N_{Noise} and small false alarm. This may be suitable to explain the degree of agreement of experiment and theory shown in Fig. 8. So we need a relative high MPPC threshold to reduce dark count rate. But it is not safe to say a larger threshold, a better MPPC performance, because the signal count rate also decreases

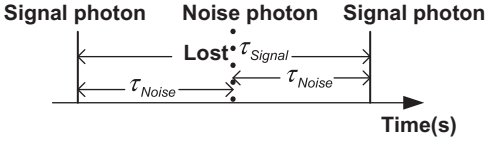

Fig. 10. Influence of a noise existence.

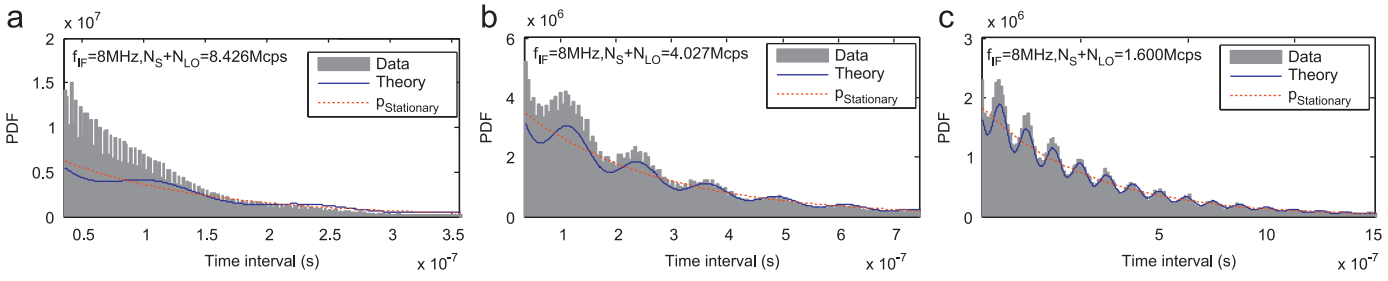

Fig. 8. Measured PDF of f_{IF}=8 MHz of various photons count rates which are about 1, 0.5, and 0.2 times the values of beat frequency.

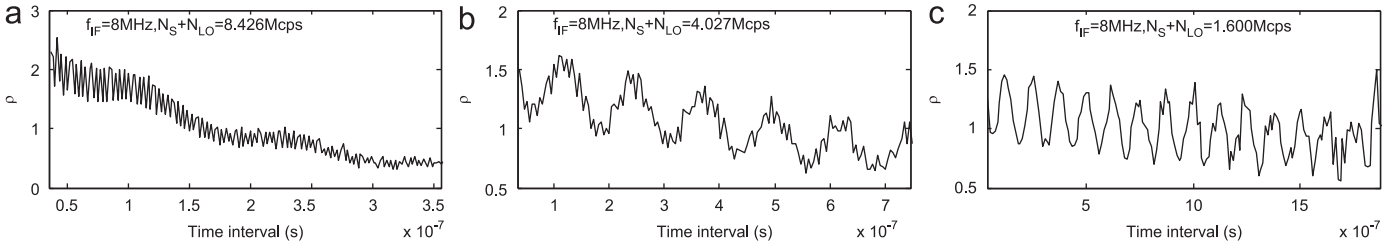

Fig. 9. The ratio of p_{Beat} to $p_{Stationary}$ in the same condition as in Fig. 8.

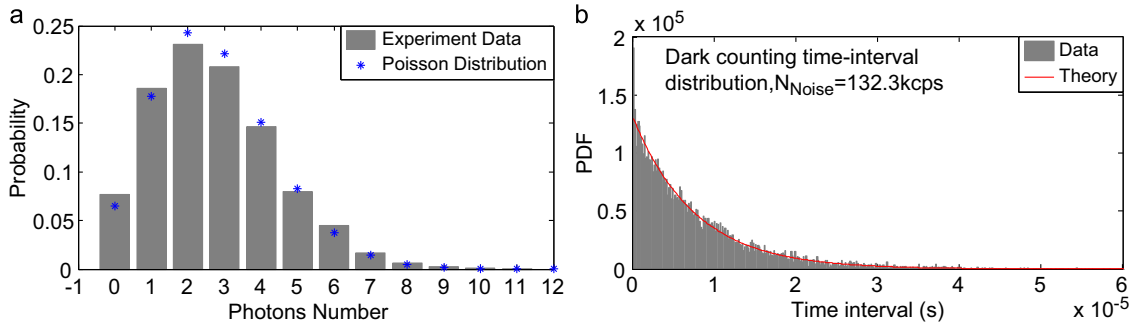

Fig. 11. (a): Dark noise probability of MPPC within 0.2 ms, it is in good agreement with the Poisson distribution. The mean noise number is 2.7325. (b): The time-interval PDF of dark noise at count rate of 132.3 kcps.

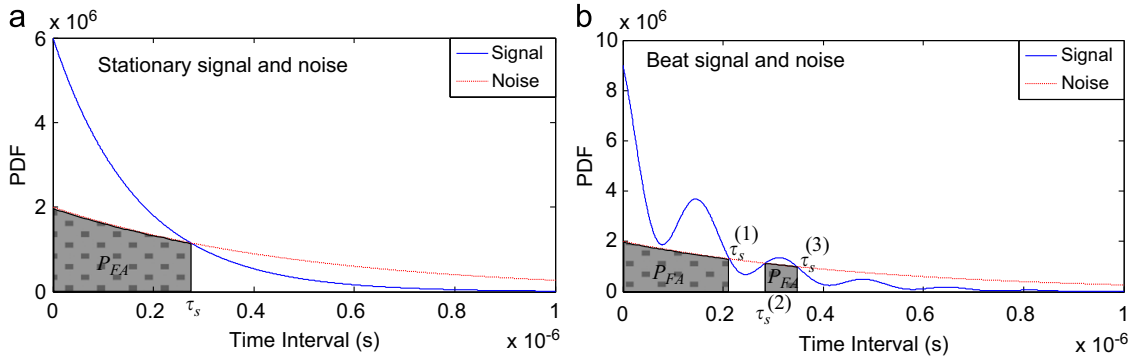

Fig. 12. The false alarm analysis of stationary (a) and beat signal (b).

Table 1
The values of N_{Noise}, N_{Signal}, N_{Signal}/N_{Noise} and p_{FA} of various MPPC thresholds.

Thresholold (p.e.)	0.05	0.075	0.1	0.125	0.15	0.175	0.2	0.225	0.25	0.275	0.3
N_{Noise} (kcps)	132.3	121.7	85.78	25.51	13.27	8.63	5.24	2.26	1.27	0.700	0.310
N_{Signal} (Mcps)	10.02	9.903	9.901	9.381	5.559	4.498	3.622	2.466	1.488	1.046	0.725
N_{Signal}/N_{Noise}	76	81	115	367	419	521	691	1091	1172	1494	2339
p_{FA} (%)	10.94	10.37	7.96	3.17	2.85	2.38	1.88	1.28	1.20	0.97	0.66

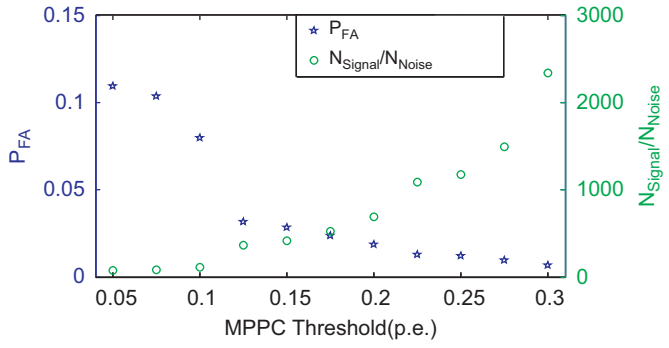

Fig. 13. The false alarm and the ratio of N_{Signal} to N_{Noise} of various MPPC thresholds.

with the rise of the thresholds (see the third row of Table 1). Especially at a very weak signal level, no signal will be detected at a very high threshold.

5. Discussion

As it is shown in Fig. 8(c) and Fig. 9(c), the time-interval PDF is in perfect agreement with the theory when the photons count rate is 0.2 times the value of beat frequency, in which condition we give another three measurements in Fig. 14. There are respectively 6, 10, and 12 fluctuation periods corresponding to time-interval of 1 μs on abscissa axis, which correspond to beat frequencies of 6, 10, and 12 MHz.

Considering the MPPC has a dark count noise of 130 kcps in our experiment, on condition that the SNR is 10, the beat signal frequency has a lower limitation of 0.433 MHz calculated by Eq. (20). So if we want to detect the lower beat frequency, the noise must be suppressed.

For MPPC, the 20 ns dead time leads to a maximum count frequency of 50 Mcps, which limits the capacity of detected beat frequency up to 25 MHz according to Nyquist criterion. But with the PDF method, we can derive the beat frequency over 25 MHz. As the former section claimed, the little photons count rate, the better performance, we give a detection result of 80 MHz beat frequency, as shown in the Fig. 15.

The theoretical calculation do not show an upper beat frequency limit even when we use a very low photons count rate, and in the experiment, we set the photons count rate to be 8 Mcps, which means the average photons number is only 0.1 in every beat period. But we still arrive at a good result, and this PDF method can surpass the dead time of the MPPC. However, the photons count rate cannot be low without a limit; the reason is the data quantity which should be enough to be processed. If the photons count rate is low, we need to detect the signal for a long

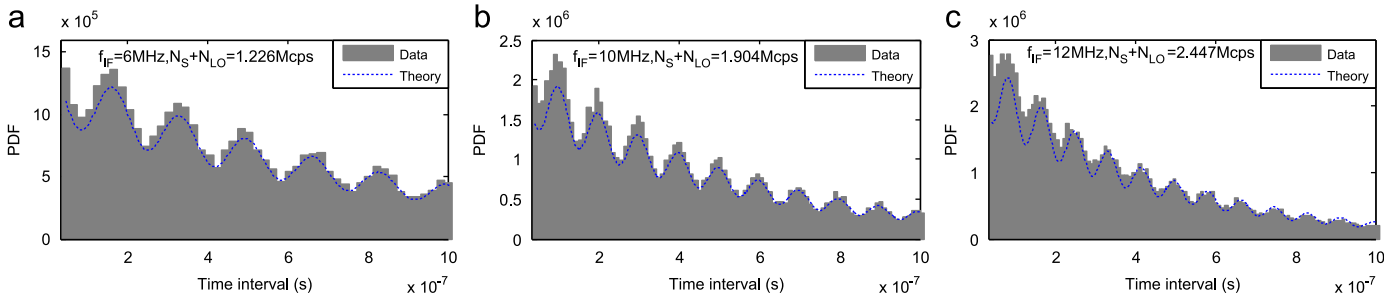

Fig. 14. Experimental PDF of various beat frequencies (6 MHz, 10 MHz and 12 MHz) when photons count rate is about 0.2 times value of frequency.

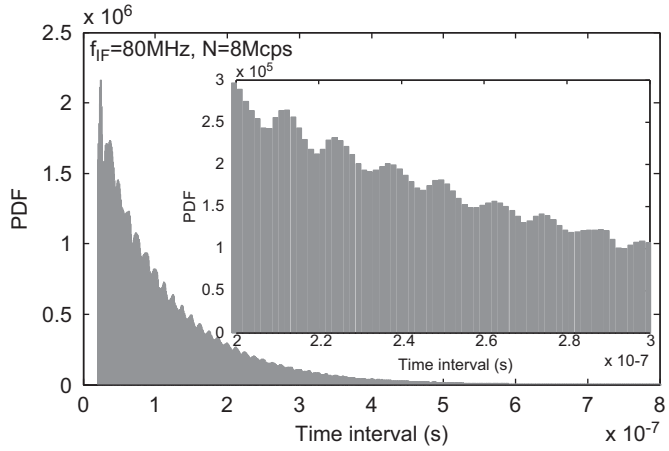

Fig. 15. Experimental PDF of 80 MHz beat frequency when photons count rate is about 8 Mcps.

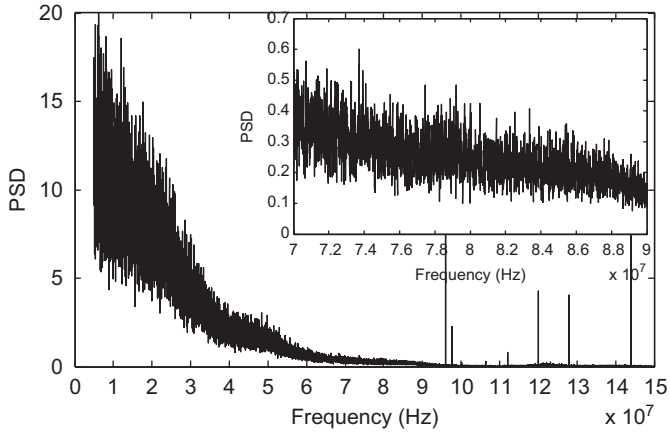

Fig. 16. The PSD of the detected signal with FFT.

time to provide enough number of time-interval. So the photons count rate must be a reasonable according to the beat frequency.

In order to illuminate the advantage of the PDF method, we give a result using FFT algorithm with the same data in Fig. 15.

From Fig. 16, there is obviously no peak value in 80 MHz, and a majority of signal is taken by the frequency within 50 MHz. The FFT algorithm hardly works when there is lower photons count rate compared to the value of beat frequency.

6. Conclusion

We present the theory to derive the photons time-interval probability density function of laser heterodyne signal, and give the experimental verification using the MPPC module to register photons arrival times. The beat frequency and mixing efficiency are both derived from the fluctuations in the PDF curve, and this is a new algorithm different from traditional laser heterodyne detection. Compared with the traditional laser heterodyne detection method, our statistics method has advantage in the condition that very low photons count rate is adopted compared to the beat frequency, and it can surpass the dead time of the detector.

Acknowledgment

This work has been supported by the Third-phase Knowledge Innovation Project of CAS in CIOMP under contract O98Y32C100.

References

[1] L.A. Jiang, J.X. Luu, Applied Optics 47 (2008) 1486.
[2] Y. Musienko, Nuclear Instruments and Methods in Physics Research Section A-Accelerators Spectrometers Detectors and Associated Equipment 598 (2009) 213.
[3] R.M. Marino, T. Stephens, R.E. Hatch, J.L. McLaughlin, J.G. Mooney, M.E. O'Brien, G.S. Rowe, J.S. Adams, L. Skelly, R.C. Knowlton, S.E. Forman, W.R. Davis, Laser Radar Technology and Applications Viii 5086 (2003) 1.
[4] M.A. Albota, R.M. Heinrichs, D.G. Kocher, D.G. Fouche, B.E. Player, M.E. O'Brien, B.F. Aull, J.J. Zayhowski, J. Mooney, B.C. Willard, R.R. Carlson, Applied Optics 41 (2002) 7671.
[5] H. Dautet, P. Deschamps, B. Dion, A.D. Macgregor, D. Macsween, R.J. McIntyre, C. Trottier, P.P. Webb, Applied Optics 32 (1993) 3894.
[6] M. Stipcevic, Applied Optics 48 (2009) 1705.
[7] D. Renker, Nuclear Instruments and Methods in Physics Research Section A-Accelerators Spectrometers Detectors and Associated Equipment 567 (2006) 48.
[8] J.X. Luu, L.A. Jiang, Applied Optics 45 (2006) 3798.
[9] E. Samain, Applied Optics 37 (1998) 502.
[10] B.A. Bushaw, T.J. Whitaker, B.D. Cannon, R.A. Warner, Journal of the Optical Society of America B-Optical Physics 2 (1985) 1547.
[11] A. Madrazo, F. Gonzalez, F. Moreno, Applied Optics 33 (1994) 4899.
[12] R. Vyas, S. Singh, Physical Review A 38 (1988) 2423.
[13] R. Vyas, S. Singh, Physical Review A 40 (1989) 5147.
[14] H.J. Carmichael, S. Singh, R. Vyas, P.R. Rice, Physical Review A 39 (1989) 1200.
[15] H. Tsuchida, Optics Letters 24 (1999) 1434.
[16] M.S. Wheatland, P.A. Sturrock, J.M. McTiernan, Astrophysical Journal 509 (1998) 448.
[17] T.A. Laurence, A.N. Kapanidis, X.X. Kong, D.S. Chemla, S. Weiss, Journal of Physical Chemistry B 108 (2004) 3051.
[18] J.W. Goodman, Wiley Classics Library, Wiley, New York, 2000.
[19] L. Lisheng, Z. Heyong, G. Jin, L. Hongbo, Z. Shuai, Optics and Precision Engineering 19 (2011) 2366.
[20] M.A. Ward, A. Vacheret, Nuclear Instruments and Methods in Physics Research A 610 (2009) 370.
[21] L. Mandel, E. Wolf, Optical Coherence and Quantum Optics, Cambridge University Press, Cambridge, New York, 1995.
[22] M. Ramilli, A. Allevi, V. Chmill, M. Bondani, M. Caccia, A. Andreoni, Journal of the Optical Society of America B-Optical Physics 27 (2010) 852.
[23] Z. Shuai, G. Jin, L. Hongbo, F. Qiang, Optics and Precision Engineering 19 (2011) 972.
[24] M. Akiba, K. Tsujino, K. Sato, M. Sasaki, Optics Express 17 (2009) 16885.
[25] G.R. Osche, Optical Detection Theory for Laser Applications, Wiley-Interscience, Hoboken, NJ, 2002.